Geological Quarterly, 2015, **59** (2): 347–357
DOI: http://dx.doi.org/10.7306/gq.1193

Shallow site investigation of Quaternary sands inside and in the vicinity of a sinkhole in the former lignite mining area in Zielona Góra (western Poland)

Waldemar S. SZAJNA[1] and Agnieszka GONTASZEWSKA[1, *]

[1] University of Zielona Góra, Institute of Building Engineering, Prof. Z. Szafrana 1, 65-516 Zielona Góra, Poland

Szajna, W.S., Gontaszewska, A., 2015. Shallow site investigation of Quaternary sands inside and in the vicinity of a sinkhole in the former lignite mining area in Zielona Góra (western Poland). Geological Quarterly, **59** (2): 347–357, doi: 10.7306/gq.1193

The paper presents a brownfield site investigation of the area where lignite was formerly exploited with an underground mining method. The Miocene lignite seams were folded by glaciers and covered with a layer of highly compacted sediments with sands on top. Yet eighty years after the extraction ceased, new sinkholes still develop. The aim of this work is to determine both the mechanical parameters of soil in the area of sinkholes and the changes in the values of these parameters induced by the process of sinkhole formation. The applied methodology involves *in situ* investigations. Soil state and strength parameters were examined with the use of CPTU and DPL tests, while stiffness parameters were determined in the SDMT test. The evaluated parameters of soil may provide data for numerical modelling of the process of sinkhole formation and may significantly simplify future *in situ* investigations in the area where the soil profile shows high natural changeability of state. The knowledge of values of parameters in a sinkhole and outside it enables easier differentiation between the zones of undisturbed soil and zones where sinkholes formed in the past (and were then backfilled) or where the sinkhole formation process is currently in progress.

Key words: sinkholes, abandoned lignite mining, *in situ* testing, soil parameters.

INTRODUCTION

The current exploitation of former industrial sites (brownfield) basically requires consideration of two problems: possible contamination of soil and water, as well as possible buried fragments of structures still remaining in the soil. In the case of underground mining terrains, old cavings and mine shafts present potential hazards of surface instabilities that may develop over such structures and in their vicinity.

The surroundings of Zielona Góra, western Poland (Fig. 1), is the region where lignite was mined for over 100 years until World War II. The lignite seams occur within a frontal moraine of the Saalian Glaciation (Warthanian Stage), which is called Wał Zielonogórski. The glaciotectonic phenomena taking place in the Pleistocene caused the lignite seams to uplift and fold. Lignite was mined down to a depth of several tens of metres, mainly in the anticlines. Currently, over eighty years after the exploitation was finished, land subsidence still occurs in this area.

Particularly dangerous forms of subsidence are sinkholes, which are discontinuous deformations of the soil surface, covering small areas. The structures may have steep or even overhung walls. The shapes of sinkholes from near Zielona Góra are usually oval in horizontal plane. Their diameters range from a few to several metres, and the average depth is a few metres. The process of their formation can be sudden.

In February 2012, three sinkholes occurred in Rybno, a hamlet in the village of Wilkanowo located west of Zielona Góra, in a close proximity to buildings. The largest one, approx. 20 m long, 10 m wide and 3–4 m deep, appeared in the location which included a local road (Fig. 2A). The time of its formation was precisely determined. The sinkhole was formed within two hours. The smallest sinkhole is circular in planar shape, with a diameter and depth of 2.5 m (Fig. 2B). This sinkhole is the subject of investigation presented in this paper.

The major causes of the formation of sinkholes are:

- the presence of a void within the soil mass (natural or anthropogenic) and its development induced by the destruction of mine casing, karst phenomena or failure of underground objects during installation, operation or after its completion;
- inconsiderable strength and rigidity of overburden;
- internal suffusion causing the outwash of small particles and the loosening of the soil structure;
- the alteration of pore pressures (seepage force, the increase in pore pressure in the soil);
- considerable loads (static and dynamic).

A sinkhole most frequently occurs when several of the factors mentioned above appear simultaneously. Due to the variety of reasons, it is very difficult to forecast the time and the place of sinkhole formation. One of the key problems for predic-

* Corresponding author, e-mail: agea.geologia@interia.pl

Received: January 22, 2014; accepted April 28, 2014; first published online: September 29, 2014

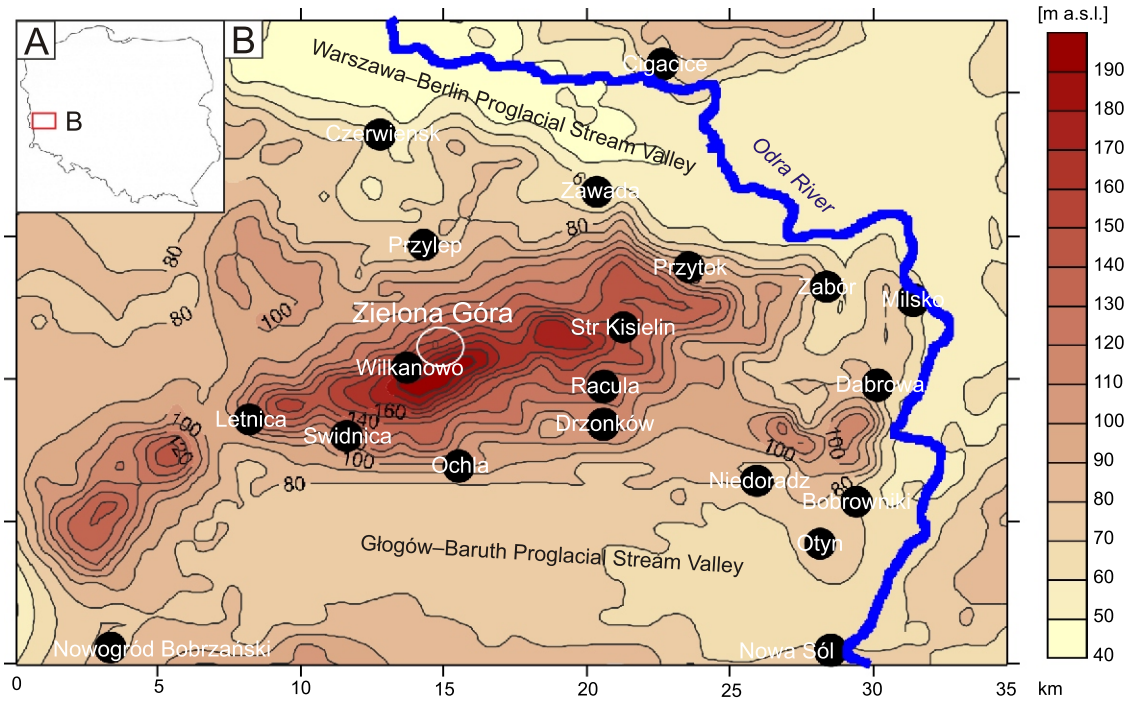

Fig. 1. Contour line map of Wał Zielonogórski

Study area marked with white circle

Fig. 2. Sinkholes at Rybno

A – largest sinkhole (western), as of February 2012,
B – smallest sinkhole (eastern), as of March 2012

tion is to recognize the mechanism of its evolution and to prepare appropriate mathematical model of the occurrence.

Land subsidence as a phenomenon has been investigated by mining engineers, geology engineers, as well as civil engineers. Despite the common objective of the investigation, i.e. the causes and forecasting of sinkhole formation, each field applies specific research methodology.

The works on mining-induced subsidence (e.g., Chudek et al., 1988; Whittaker and Reddish, 1989; Singh and Dhar, 1997; Pilecki and Kotyrba, 2007) focus on the determination of depth and exploitation methods as well as the manner of liquidation of workings, tunnels and shafts. The stress is put on the significance of geophysical investigations allowing the determination of the underground voids. Thomas and Roth (1999) present additional evaluation of invasive investigation methods. Drilling and static probing CPT (cone penetration test) have been given the highest notes.

There is a large number of publications on the study of karst sinkholes in areas of non-rock overburden (e.g., Chang and Basnett, 1999; Kannan,1999; Waltham et al., 2005; Gutierrez et al., 2008). Waltham et al. (2005) attempted to link the morphology of sinkholes with the causes, time and rate of their formation. They suggested that cylindrical sinkholes were formed in soils with cohesive overburden due to soil collapse into voids and develop within minutes, whereas conical-shaped sinkholes, characteristic for the area of non-cohesive overburden, resulted from internal suffusion and develop slowly (months or years). The described research methods were limited to geophysical studies which traced underground voids. Kannan (1999) and Chang and Basnett (1999) discussed the utilisation of invasive methods SPT (standard penetration test) and CPT for the investigations of sinkhole areas.

Specialists in soil mechanics have also been involved in the investigation of the mechanisms of sinkhole formation, almost since the first stages of this branch of science. Terzaghi (1936) carried out experimental and analytical studies of changes in

the state of stress in loose soils above a trapdoor, defining the phenomenon of arching. Newer model studies conducted on centrifuges (e.g., Craig, 1990; Iglesia et al., 1990; Abdulla and Goodings, 1996; Costa et al., 2009) enabled a better understanding of the mechanism of sinkhole formation and implicated the application of another scientific area, i.e. analytical and numerical modelling, for sinkhole analysis (e.g., Tharp, 1999; Ambrozić and Turk, 2003; Augarde et al., 2003).

Having discussed the approaches to the investigations of sinkhole areas, the attention will be now drawn onto the subject of this research. The method of operation used in Zielona Góra lignite mines (within the German borders before World War II) has been described on the basis of archival materials, incomplete though, in the work of Gontaszewska and Kraiński (2012). The average depth at which lignite was extracted was 20–40 m, galleries were 1.5 m wide and 2 m high, and the area of typical extraction chamber was 4–5 m^2 with the height of 3–4 m.

Geophysical tests MASW (multichannel analysis of surface waves), carried out on the discussed area by a commercial company, described in part by Szajna (2013), did not show clearly the existence of voids, while they indicated zones of probable ground loosening. These zones are the subject of the invasive tests described in this paper.

Natural undisturbed soils demonstrate considerable changeability of features and state parameters, especially the ones of glacial origin. This changeability impedes the investigations, including the identification of sinkhole-caused loosening zones. It refers to the identification of both old backfilled sinkholes which are not revealed by the morphology of the area, and new ones which are in the process of formation. In this context, an important question arises: how the formation of sinkholes influences the change in the values of soil parameters?

GEOLOGICAL SETTING

Zielona Góra and its surroundings were the areas of lignite mining for more than 110 years. A ten-odd of lignite mines, mostly underground, operated in the area. The oldest and the greatest venture was the “Consolidierte Grünberger Gruben” company operating until the end of World War II. Mining was concentrated mainly west of Zielona Góra, within the villages of Wilkanowo–Słone–Letnica, and in the western periphery of the town (Bujkiewicz, 1997; Gontaszewska and Kraiński, 2010, 2012; Gontaszewska, 2011). The location and the morphology of the discussed area are shown in Figure 1.

The available German materials, incomplete though, include mining maps in the scale of 1:1000 (from the 1930s) and annual reports from 1923–1940.

This paper refers to the area adjacent directly to the town, i.e. the hamlet of Rybno, belonging to the village of Wilkanowo. The study was conducted at the premises of Zielona Góra Forestry Administration.

Today’s Rybno is among the first mining areas near Zielona Góra. The exploitation took place on both sides of the Wilkanowo – Zielona Góra road, and the four lignite seams stretched parallel to that road (as seen in Fig. 3). The mining was carried out in stages within the period 1853–1929 in anticlinal parts of folds. Parts of synclines with possible lignite deposits are located to the south and north of the seams. Directly to the west of the shafts, there was a glass works that operated in the area. It is still possible to find production wastes, including slag and glass lumps, at numerous places. They were also used to backfill the mine shafts and land subsidence.

Site research described in this paper was carried out on the Hütten seam. The seam was exploited in the years 1870–1878 and again from 1922 to 1925. The shaft was built in 1922, and it was 26 m deep. The lowest mining level (127.2 m) indicates that the extraction reached a depth of about 40 m. The lignite was not mined under the buildings of the glass works (safety pillar).

The relatively shallow occurrence of lignite in the Zielona Góra area is related to the structure called Wał Zielonogórski (Fig. 1). It is a moraine formed during the Warthanian Stage and composed of layers of Miocene and older Pleistocene deposits. The lignite seams occur in glaciotectonically disturbed deposits of the Wał Zielonogórski, together with the Poznań Formation

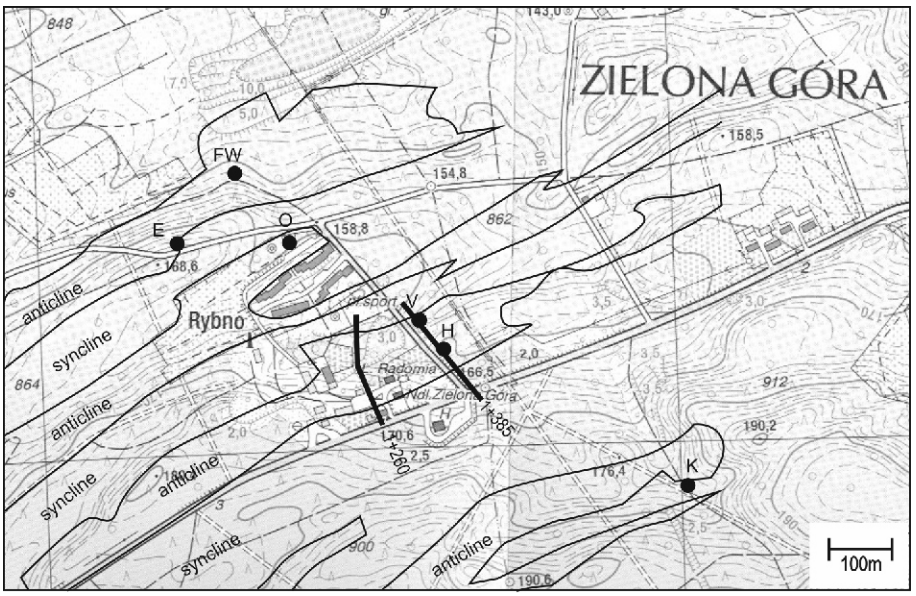

Fig. 3. Current map of Rybno hamlet with approximately indicated exploitation regions

Mining shafts are marked with dots: E – Emilie, FW – Friedrich Wilhelm, H – Hütten, O – Otto, V – Versuch, K – Krug von Nidda, and lines of archival maps

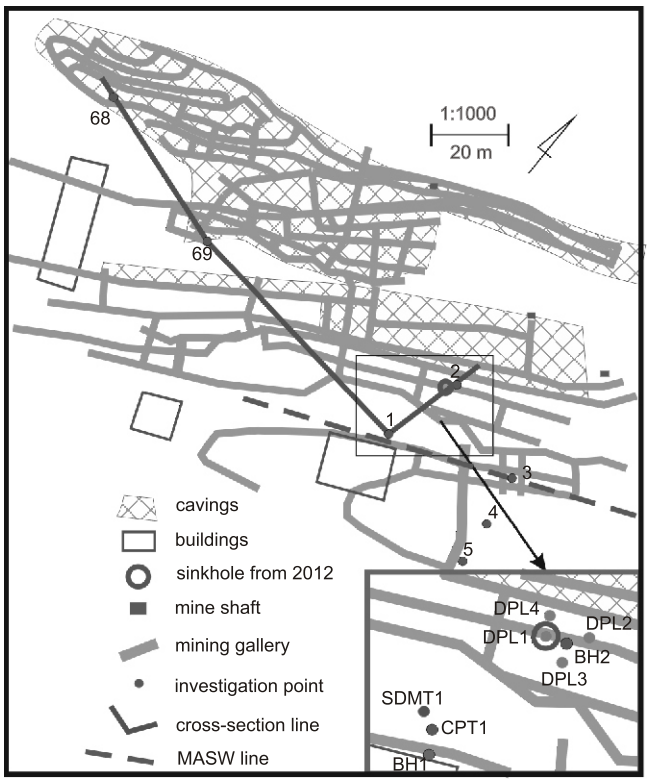

Fig. 4. Map of the investigated area

BH – borehole, CPT – cone penetration tests, DPL – dynamic probing light, SDMT – seismic dilatometer test

clays. Lignite was mined mainly in anticlines and descended to the depth of the groundwater table, although generally not deeper than 50 m.

The lignite overburden contains Pleistocene formations and blue and grey clays of Poznań Formation. The thickness of the lignite is inconsiderable, typically of 3–4 m. The lignite floor consists of grey clays with quartz sands below. The age of the lignite is determined as the first group of lignite layers – Middle Miocene.

The map of the investigated area is presented in Figure 4. Archival boreholes and the geological cross-section are marked on the map. The cross-section goes through the points 68-69-1-2. The map also shows cavings, locations of the eastern borehole as well as the investigation points described in further chapters.

The geological structure of the described area does not deviate from the above pattern. The Upper Miocene is represented mainly by clays with inserts of silt and sand, containing a lignite seam. Above it, there are Pleistocene boulder tills of the Warthanian Stage under a cover of sandy and gravel sediments of the Vistulian Glaciation, as shown in a cross-section (Fig. 5). As a result of glaciotectonic disturbances caused by Warthanian Stage, these sediments were folded or even over-folded.

In the Rybno area, there are two overthrust faults: southern fault mined with the Hütten and Versuch shafts, and northern one exploited with the Otto shaft (Fig. 3). N–S cross-sections through the southern overthrust faults (Hütten seam) are shown in the original German map (Fig. 6).

The lignite seam in the overthrust faults was uplifted to the elevations of around 132–154 m above the sea level (about 11–50 m depth). Both overthrust faults are separated by deep anticlinal zones filled with glaciofluvial sand and gravel deposits. On the basis of deep drillings, the depth of the synclines may be estimated at least at 50 m.

Virtually, the terrain deformations are found over the entire area of the former lignite mining. Most frequently, they are now conical-shaped forms (particularly in the regions of the earliest exploitation in the 19th century) with longitudinal depressions that developed over the galleries. There were also reports of the formation of sinkholes, usually cylindrical in shape. In the 1970s, a sinkhole of several metres in diameter appeared in the area of neighbouring village of Buchałów (Szafran and Wróbel, 1975), where most probably one of the shafts, which operated on the “Schloin” seam, fell in. In 2005, a sinkhole of a few metres in diameter appeared in the place of the ventilation shaft at the “Pohlenz” seams.

Terrain deformations that have occurred in this area are closely related to the method of lignite exploitation. The seam was approached from vertical shafts, tunnels and inclined shafts conducted from the surface. The exploitation was carried out in horizontal galleries parallel to the seam, thus the galleries descended gradually deeper and deeper. The lignite was mined with a collapse method. Wooden casings were partially or completely removed after the mining was finished, whereas the shafts were backfilled. Depending on the type of the overburden (sand, clays or tills), the collapse of the roof and the appearance of surface deformations lasted several years. Deformations had certainly appeared yet when lignite was still mined, which may be concluded from the fact that a protective pillar under the glass factory was established in 1924 (two years after mining was started; now the offices of the Forestry; Betriebsbericht, 1931).

The documentation of the Forestry buildings (Gontaszewska and Kraiński, 2012) describes the appearance of a new sinkhole in the place of a borehole, where no evidence of voids or exploitation was found. Another borehole revealed a 14 metre layer of slag, however not drilled through. It may be concluded that it was a former backfilled caving.

The greatest deformation at Rybno, elongated funnel in shape, is located directly to the north of the Forestry offices, in the place where almost a vertical limb of the anticline was exploited, which is visible on the profile 1+385 (Fig. 6). Total thickness of the extracted lignite can be estimated at about 12–14 m, and the maximum depth of the sinkhole is about 6 m.

In February 2012, at a time of intense frost, three new sinkholes appeared at Rybno (Fig. 2). The largest sinkhole, about 20 m long, approx. 10 m wide, and 3–4 m deep, appeared in the protection pillar area. The locations of the sinkholes are shown on the mining map (Fig. 7). They do not coincide with any of the shafts, which was the case in the previous sinkholes. The causes of the development of these deformations are difficult to explain. The sinkhole in the eastern part, which developed on the Forestry grounds (Figs. 5 and 7), may be associated with the repeated exploitation in 1923 at a depth of about 21 m, in the area exploited already in 1870. However, there is no data on the earlier exploitation.

The origin of the two remaining sinkholes, which developed in the western part of the Forestry premises, is much more difficult to analyse and explain. They both developed over the galleries performed between 1923 and 1925, but they are located on the area which was most likely exploited after this date. In addition, the largest sinkhole is located over the northern end of the north-south-oriented gallery marked on the map as “Zieh-Scht.”. It could be a transport shaft (or an inclined shaft) backfilled only in the subsurface part. This “cork” may have slidden down along the shaft, which eventually resulted in the formation of the sinkhole.

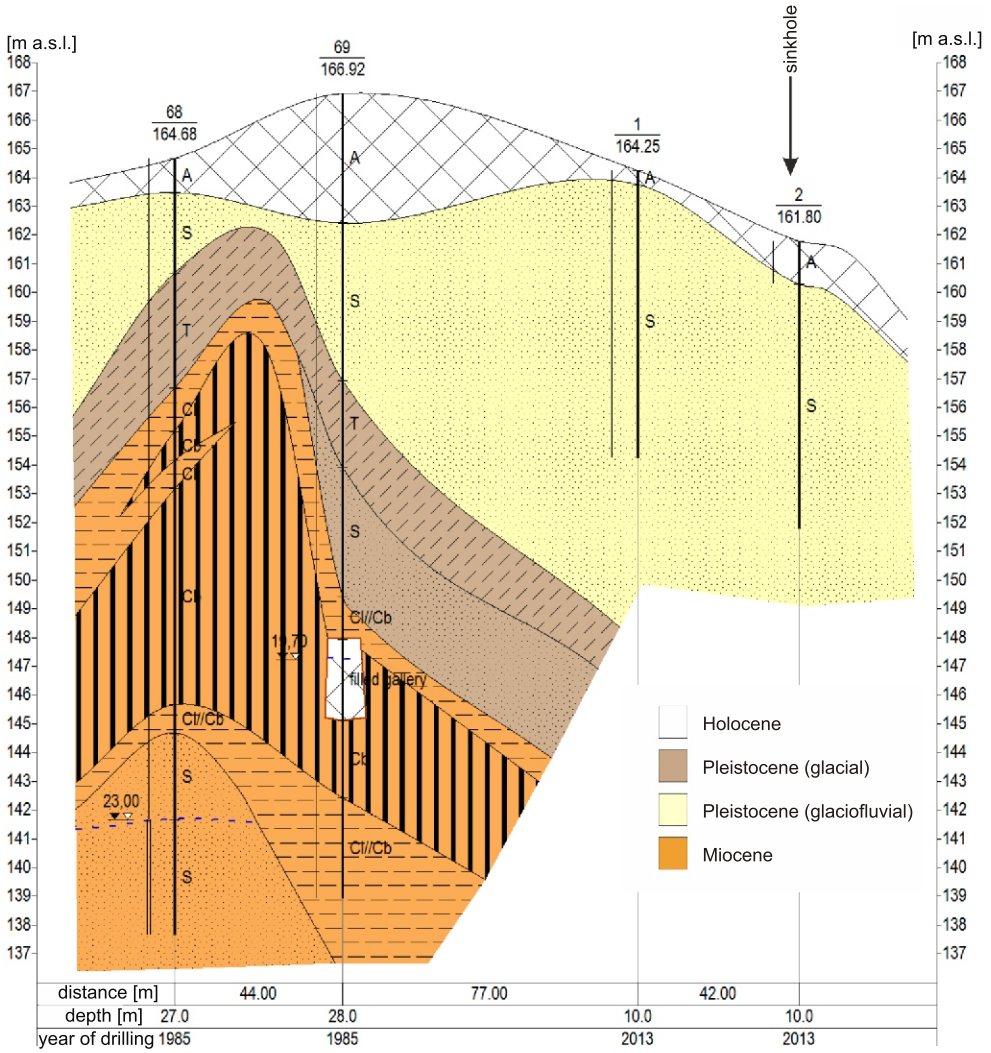

Fig. 5. Geological cross-section through the investigated area

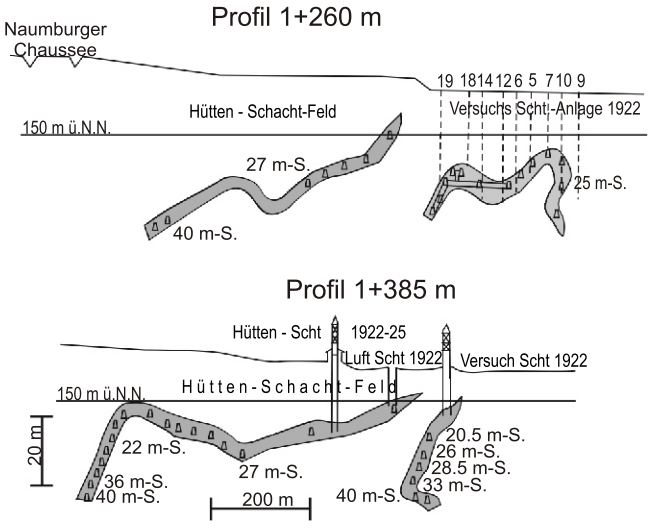

Fig. 6. A sketch of original mine profiles

The locations of cross-sections are shown in the map; mine galleries are marked; 40 m-S refers to a seam at a depth of 40 m

THE SELECTION OF INVESTIGATION AREAS, SUITABLE PARAMETERS AND RESEARCH METHODS

Sinkholes that developed at Rybno in February 2012 appeared rapidly. Both the size (the largest sinkhole was approximately 20 10 m in projection and 3–4 m deep) and the short formation time (within 2 h) aroused fears of further possible land subsidence, which may threaten the existing buildings. Accordingly, the plan of investigations included subsoil tests carried out in five areas (Fig. 4). The results of two of them, i.e. in the vicinity of buildings and in the sinkholes and their surroundings, are presented in details in the paper. The largest sinkhole (western) developed under a paved road (Fig. 2A). It prevented from invasive testing of this sinkhole, for the concrete bricks could damage the test equipment. Thus, the eastern sinkhole was selected as the subject of investigations (Fig. 7).

The area is owned by the State Forestry Administration. As suggested by its employees, the area has declined near one of the buildings, so the research was started in the vicinity of that building. Fears that sinkholes may develop in this area were justified by the layout of the galleries in old maps (Fig. 7), and by the mentioned MASW investigations. The building, location of

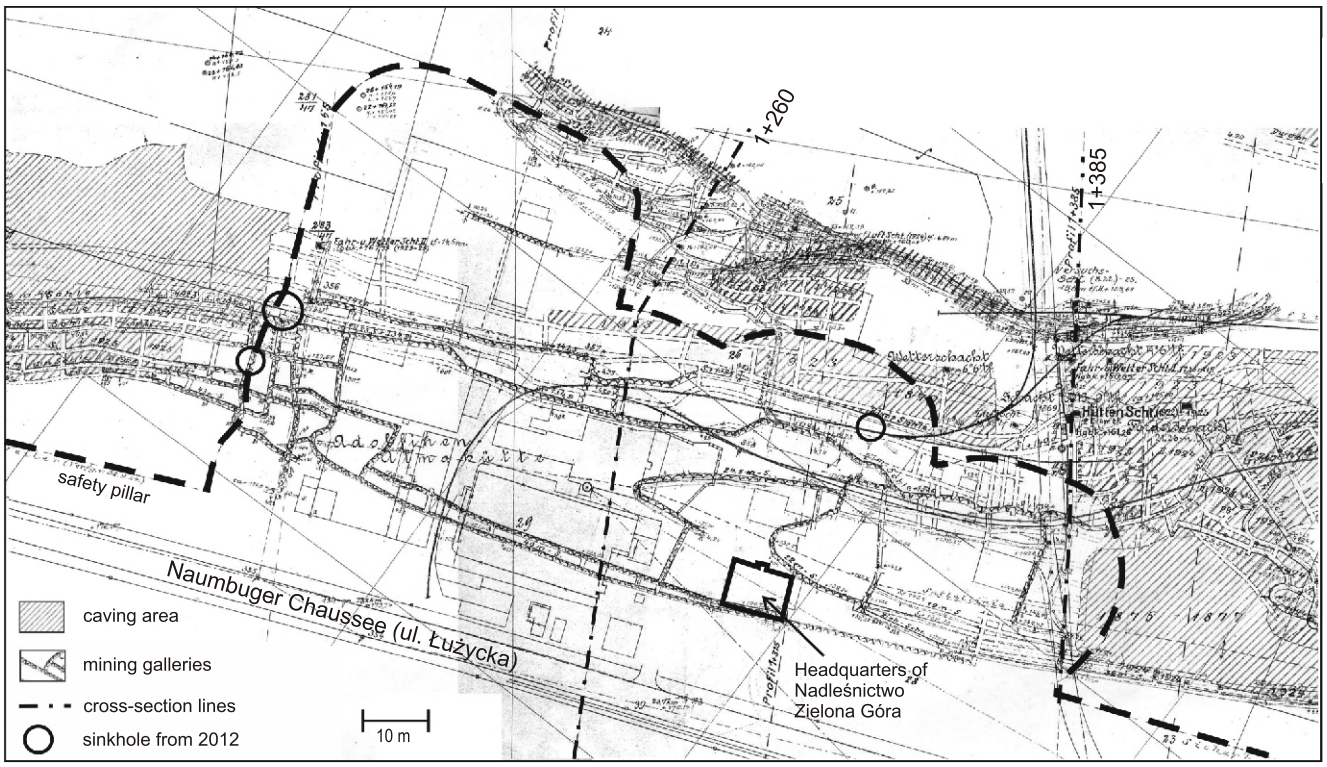

Fig. 7. Mining map of the Hütten seam, approx. 1940, with marked sinkholes from 2012

the galleries and the MASW test line, and the individual research points are shown in Figure 4.

The area of subsequent research was the eastern sinkhole and its vicinity. In order to compensate for the land cavity, the sinkhole had been backfilled with non-cohesive soil without compaction a year before. The location and the particular investigation points are also presented in Figure 4.

The substantial objective of the investigation is the determination of the stiffness of the soil and its state and strength parameters. The geological study indicated that the soil under a slag embankment consists of non-cohesive material, mainly fine sands. The basic parameter of state for sand is relative density index (I_D). The Mohr-Coulomb model, a parameter of which is the effective friction angle (’), has been assumed as a strength model. Stiffness parameters to be determined are the constrained modulus (M) and initial shear modulus (G_0).

Due to the difficulties in receiving undisturbed sand samples for triaxial tests, mechanical parameters of soil have been determined by *in situ* tests. Lunne (2001) and Mayne et al. (2009) evaluated various apparatuses for determination of soil parameters. They concluded that for the described soil conditions, CPTU (CPT with pore water pressure measurement) is best suited for strength parameters determination, whereas SDMT – for stiffness parameters determination. Both apparatuses were applied in the presented investigations. The points marked in Figure 4 refer to the places where probing was performed with the use of a piezoelectric cone (CPTU) and a seismic dilatometer test (SDMT).

The tests used a rig of 100 kN maximum allowable trust, mounted on a track of 1 tonne total deadweight. Due to the existence of non-cohesive industrial waste (slag with large lumps of glass) in the superficial zone, helical anchors were used for stabilization.

Sinkhole investigations started in the central part of the eastern sinkhole with the use of SDMT. The penetration with the dilatometer blade was carried out down to a depth of 4 m, i.e. 1.5 m below the bed of the sinkhole, and then it was stopped. The values of soil resistances were too low for p_0 to be read. At the same time, the glass lumps caused damage to the membrane of the SDMT blade. In addition, the vibrations of the rig generated during the penetration threatened a collapse of the track and caused the compaction of the examined soil. In the view of the occurred difficulties, further studies were performed with the use of the light dynamic probing light test (DPL). The locations of particular DPL test points are shown in Figure 4.

In the CPTU test, a conical tip with a cylindrical sleeve of 35.7 mm in diameter is pushed into the ground at a constant speed of 2 cm/s (e.g., Lunne et al., 1997). The following parameters are measured: cone resistance (q_c), sleeve friction (f_s) and pore pressure (u) induced by the cone penetration. However, none of the measured values is a strength parameter. Thus, in order to determine the soil strength (angle of internal friction), the correlation equations should be used.

A similar situation occurs in the case of DPL tests, during which the conical tip is immersed dynamically, and the result of the measurement is the number of blows per 10 cm penetration (N_{10}). Also in this case, the soil state parameters, such as the degree of compaction I_D, may be determined only with correlation equations.

Correlation equations used for the interpretation of CPTU and DPL tests are valid only for specific types of soil. Admittedly, for CPTU investigations, the type of soil may be estimated on the basis of the measured values of q_c and f_s. However, two additional boreholes (BH1 and BH2; Fig. 4) were performed and samples were taken in the vicinity of both tests. Thus, the type of soil was determined on the basis of grain-size analysis.

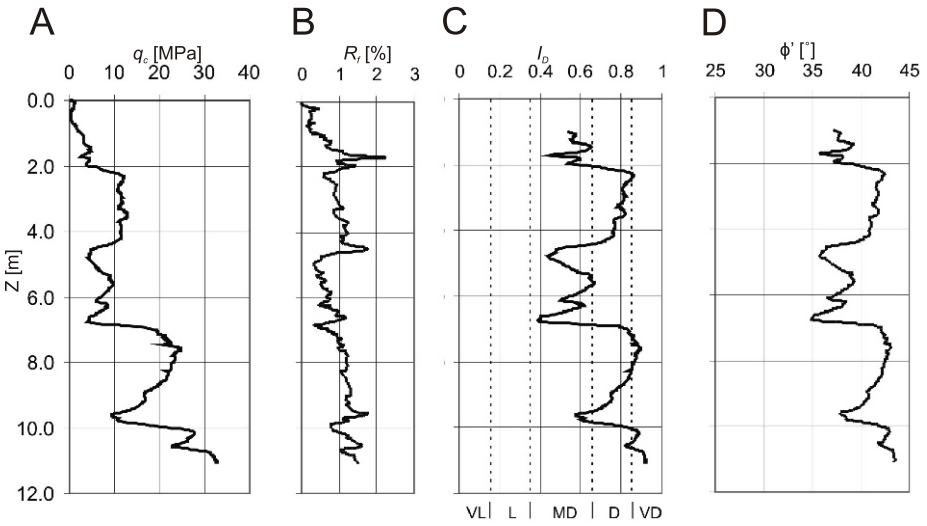

Fig. 8. Results and interpretation of the CPT1 test

A – cone resistance (q_c); **B** – friction ratio (R_f); **C** – index of density (I_D); **D** – effective friction angle ('); VL – very loose, L – loose, MD – medium, dense, D – dense, VD – very dense, *Z* – depth

An SDMT test actually consists of two types of independent tests. The first type is a standard (DMT) flat dilatometer test (e.g., Marchetti et al., 2001), during which pressures causing horizontal deformation of the membrane, which is immersed in soil, are measured, i.e. contact pressure (p_0) and expansion pressure (p_1). The second type of test involves measurement of the velocity V_S of transverse waves generated on the surface and recorded by the geophones mounted above the dilatometer blade.

TEST RESULTS AND PARAMETER INTERPRETATION

The applied research methodology does not allow obtaining the values of strength and stiffness parameters directly. In order to obtain the values, the test results need to be interpreted with the use of suitable correlation equations, which are presented below. The presentation and interpretation of the recorded values will first refer to the tests carried out in the vicinity of the building (investigation point 1 in Fig. 4), and then – to the tests of the eastern sinkhole (investigation point 2 in Fig. 4).

Figures 8A and B show the results of static probing performed in the vicinity of the building, marked as CPT1 (Fig. 4). The figures show the results of measurements of cone resistance (q_c) and friction ratio ($R_f = f_s/q_c$). This is a standard way of result presentation of CPTU tests, where parameter q_c is a good measure of the soil state, and R_f indicates the type of tested soil. Due to the low groundwater table level within the studied depths, parameter $u = 0$.

In order to interpret the results of CPTU test, the type of soil should be determined. On the basis of nomograms proposed by Robertson in 1986 (e.g., Lunne et al., 1997), the soil type was determined to fall within the limits from sandy silt to sand. Granulometric tests of samples from borehole BH1 showed that the grading of the tested soil ranged between silty sand with gravel and sand.

Index of density I_D was determined from a correlation equation for sand, proposed by Lancellotta (2009):

$$I_D \quad 0.268 \ln \frac{q_c / p_{atm}}{\sqrt{'_{v0}/p_{atm}}} \quad 0.675 \qquad [1]$$

where: $'_{v0}$ – an effective normal vertical stress, p_{atm} – an atmospheric pressure. The determined value of the degree of compaction is presented in Figure 8C.

Effective friction angle ' was also determined from the correlation between this value and the measured parameter q_c, proposed by Mayne (2007):

$$' \quad 17.6 \quad 11 \log \frac{q_c}{\sqrt{'_{v0} p_{atm}}} \qquad [2]$$

Figure 8D presents the values of internal friction angle at particular depths.

To determine soil stiffness parameters for investigation point 1 (Fig. 9) SDMT1 test was performed. Figure 9A presents the recorded pressures p_0 and p_1. Based on the solution to the problem of a circular plate pushed into an elastic half-space (Marchetti, 1980), the constrained modulus (*M*) may be determined (e.g., Marchetti et al., 2001):

$$M \quad 34.7 \; p_1 \quad p_0 \; R_M \qquad [3]$$

where: R_M – a correlation function dependent on the soil type and the p_0 and p_1 values.

The obtained values *M* are shown in Figure 9B.

During the seismic dilatometer test in point SDMT1, values of shear waves velocity V_S propagating in the subsoil were also measured. The recorded values are presented in Figure 9C. Since the soil vibrations during seismic tests occur for very small deformations, the velocities of waves may be transformed into values G_0 as for an elastic medium (e.g., Lancellotta, 2009)

$$G_0 \quad V_S^2 \qquad [4]$$

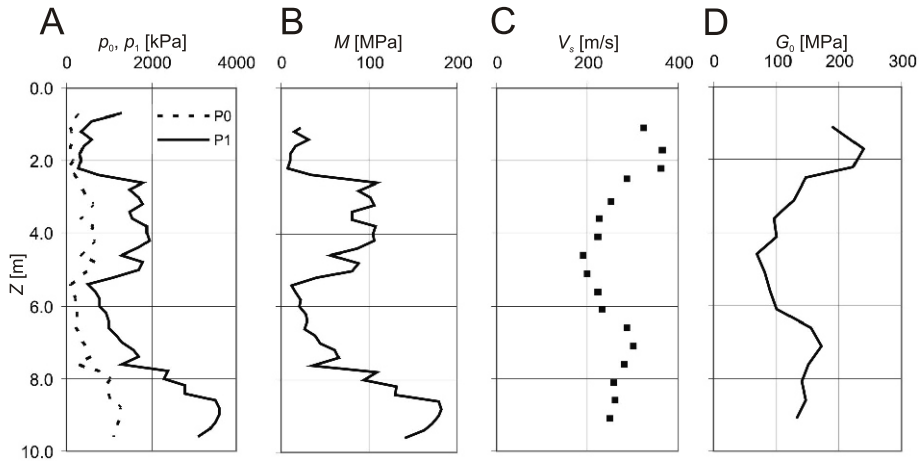

Fig. 9. Results and interpretation of the SDMT1 test

A – contact pressure (p_0) and expansion pressure (p_1); **B** – constrained modulus (M); **C** – shear waves velocity (V_S); **D** – initial shear modulus (G_0)

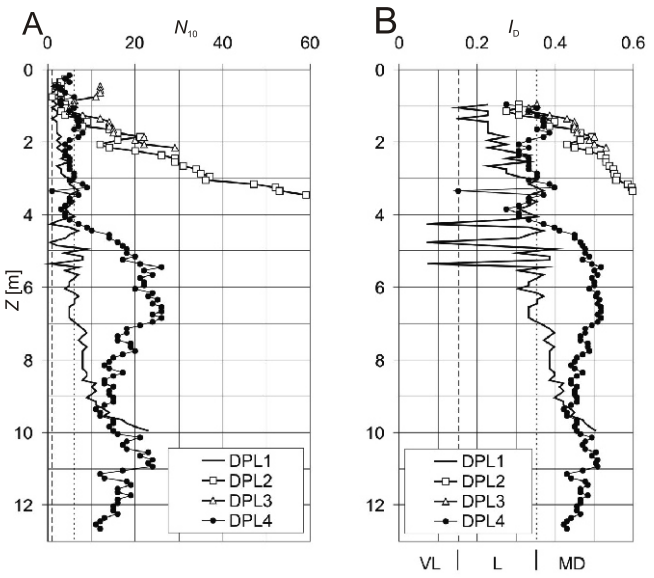

Fig. 10. Results and interpretation of DPL tests in the sinkhole and in its vicinity

A – number of blows per 10 cm penetration (N_{10}); **B** – index of density (I_D); explanations as in Figure 8

Table 1

Soil description and results of particle size analysis

Layer	Z [m]	Type (ISO)	Colour	C_U	C_C
1	1.5–2.0	FSa	cream	2.25	1.25
2	2.0–2.9	grCSa	brown	3.06	1.00
3	2.9–6.5	FSa	yellow	1.57	0.96
4	6.5–9.8	FSa	orange	1.58	0.96
5	9.8–10.0	FSa	cream	1.53	0.96

C_U – uniformity coefficient, C_C – coefficient of curvature

whereas the subsoil density may be determined by the correlation 8.64 logV_S 0.74 log $'_{v0}$ 0.4 /9.81 (Mayne et al., 2009). The solid line in Figure 9D demonstrates the values of shear modulus determined in SDMT tests.

A different testing method was applied in the soil examination in the eastern sinkhole (investigation point 2 in Fig. 4). Due to the difficulties in carrying out the SDMT tests discussed above, DPL tests were performed. To determine the state of soil in the sinkhole, a probing was performed in its central part, denoted as DPL1. Two more tests were also performed in its vicinity, marked as DPL2 and DPL3, in order to compare the state of soil before the sinkhole formation. The fourth test, DPL4, was carried out between the northern edge of the sinkhole and the old sinkholes formed before 1984 (probably in the first half of the 20th century). The southern outskirts of the area of old sinkholes currently form a slope inclined to the north. The DPL4 test was performed at a distance of 1 m from the edge of the sinkhole of 2012 and approximately 1 m from the edge of the before-mentioned slope. The measured values of N_{10} for each of the tests are shown in Figure 10A.

The interpretation of DPL tests requires the determination of particle size of the tested soil. For this purpose, a borehole (down to a depth of 10 m) was drilled (named as BH1), and then a granulometric analysis was made. While drilling, five separate soil layers were identified. The characteristics of particle size in the form of uniformity coefficient (C_U) and curvature coefficient (C_C) are shown in Table 1.

The granulometric analysis revealed that the grading parameters of the last three soil layers shown in Table1 practically coincide, and the only discriminating factor in the macroscopic analysis was the colour. Thus, grading curves are shown (Fig. 11) only for the first three soil layers, namely for depths of 1.75, 2.5 and 4.0 m.

Having known the characteristics of particle sizes and the values N_{10}, the degree of the compaction of soil overlying the groundwater table has been calculated with the correlation proposed by Stenzel and Melzer (1978):

$$I_D \quad 0.15 \quad 0.26 \log N_{10} \qquad [5]$$

The obtained relative density values for each individual probing are shown in Figure 10B.

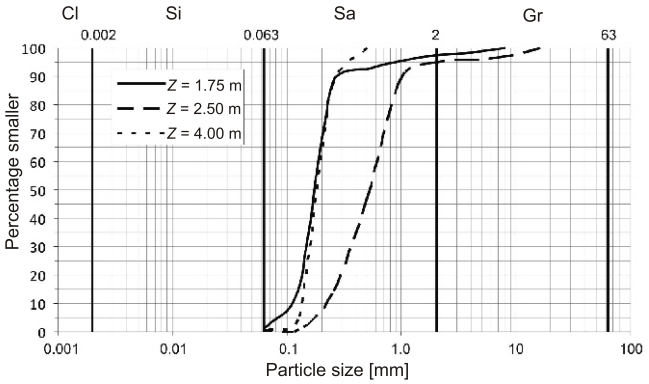

Fig. 11. Sieving curves for soil from borehole BH2

Cl – clay, Si – silt, Sa – sand, Gr – gravel

DISCUSSION OF RESULTS

The index of density of sand, obtained from CPT1 test and presented in Figure 8C, shows that the state of soil is not worse than "medium dense" to a depth of 11 m. The state of the superficial layer, to a depth of 1 m, which is formed by slag filling, is impossible to interpret because there are no suitable correlation formulas for such material. In the zone of 2–4 m, the soil is in a "dense" state (D), and at a depth of approx. 8 m and below 10 m – even in a "very dense" state (VD). The high value of index of density of glacial sands caused that it was impossible to continue probing at depths greater than 11 m, using the 100 kN rig and the anchoring system. The main obstacle was the filling (note low values of q_c to a depth of 1 m in Fig. 8A) consisting of slag with glass lumps, which caused considerable frictional resistance during anchoring, and a small load capacity of the anchor. The low weight of the track also plays a significant role.

The tested soil, due to a significant density, is characterized by high values of internal friction angle shown in Figure 8D, which means that it reveals high strength under drained loading conditions. In particular, within a depth of 2–4.5 m and below 7 m, the angle ' exceeds 40° in almost the entire range. At this point, it is worth mentioning that the correlation equation used to determine the friction angle has been derived for the medium completely saturated with water and thus, for unsaturated sand, the capillarity forces induce certain overestimation of the obtained strength.

Analysing the stiffness of the soil, it may be seen in Figure 9B that the constrained modulus (M), obtained in the SDMT1, takes considerable values of the order of 100 MPa at a depth ranging from about 2 to 5 m. Below a depth of 8 m, the M value is much greater, attaining 180 MPa at a depth of approximately 9 m. Low constrained modulus was recorded for depths of 2 m and 5.4 m, and it ranges from 8 to 12 MPa, respectively.

The comparison of results of CPT1 and SDMT1 tests in the ranges discussed above, gives a consistent picture of the soil reaction on test load. The shapes of curves representing the values p_0 and p_1, shown in Figure 9A, are similar to the shape of q_c, presented in Figure 8A. Low values are recorded for depths to about 2 m and then between 5–7 m, whereas high values are recorded for depths between 2–5 m and 7–9 m.

The picture of soil stiffness becomes much more complicated when considering the results of seismic SDMT1 tests (Fig. 9D). At a depth of approximately 2 m, the module G_0 reaches its maximum values whereas its minimum falls at a depth of approximately 4.5 m. The obtained values of shear modulus do not fit the results of constrained modulus (M). This inconsistency is difficult to explain and would require additional studies.

At the end of this part of discussion, it should be stressed that the SDMT1 tests were performed only to a depth of 9.6 m. The reasons are just the same as in the case of CPT1 tests and are described in the first paragraph of the current section. It is estimated that the soil resistance induced by pressing the dilatometer blade into the soil is about 10–30% higher than the resistance resulting from the standard cone penetration.

Interesting results are obtained for a dynamic probing light test carried out in the sinkhole itself and in its immediate vicinity. The results of DPL1 test (Fig. 10), to a depth of 2.5 m, refer to a backfilling made in 2012 after the sinkhole formation. Below this depth, down to 7 m, the soil is in the "loose" state. In this zone, at depths of 4–5.5 m, it is likely to find voids or unstable soil structures, as a single dynamic probe impulse caused the device to go into the soil by several centimetres. Due to the difficulties in the precise determination of the number of strokes per 10 cm cone movement at these depths, it was assumed that N_{10} = 0.5. Below a depth of 7 m, the soil is in a "medium dense" state.

The following two tests, i.e. DPL2 and DPL3, were performed in the area which does not demonstrate any former land subsidence, and the soil is in an undisturbed state. The value of N_{10}, obtained in the DPL2 test at a depth below 3 m, exceeds 50 and prevents reliable interpretation in this type of study (Fig. 10A). DPL3 test was performed to verify the results obtained in test DPL2 and confirms the previous results. Both tests suggest that below the slag embankment, N_{10} values are distinctly higher than the values obtained in the DPL1 test and the sand is in a "medium dense" state.

The DPL4 test was performed to verify the state of soil in the place between the sinkhole formed in 2012 and the one formed before 1984. As shown in Figure 10A, the results of DPL4 and DPL1 tests overlap down to a depth of 4.5 m. In the case of DPL4 test, N_{10} valued zero at a depth of 3.3 m. A certain difference in the recorded values occurs at depths ranging from 4.5 to 8 m. Below 8 m, the results of both tests overlap again. A comparison of the graphs shows that despite the absence of deformation on the surface within the area of DPL4 test, the state of soil is similar to that in the sinkhole. This may suggest that the loosening of the soil caused by sinkhole affected the subsurface of this area as well. An alternative hypothesis is also possible, i.e. the loosening may be caused by an old sinkhole. In this case, it would mean that the newly formed sinkhole is just another phase of the sinkhole process that started in this region in the 20th century.

SUMMARY AND CONCLUSIONS

The paper presents the results of brownfield site investigation. The area was examined due to numerous sinkhole appearances. They are attributed to former underground lignite mining which was stopped 80 years ago. Despite the extraction ceased, sinkholes still develop in this area threatening the existing buildings and people. The main aim of this work was to determine the state parameters, i.e. strength and stiffness of the soil, in the area where sinkholes developed, and to determine the changes in the values of these parameters induced by the process of sinkhole formation.

Soil strength parameters in the vicinity of the building were determined with the use of cone penetration test (CPTU), and

stiffness parameters – with the use of seismic dilatometer test (SDMT). This methodology could not be applied inside the sinkhole, due to the soil condition. In the sinkhole and its vicinity, light dynamic probing tests (DPL) were performed.

CPTU and SDMT tests carried out in the vicinity of the building allowed the determination of the index of density, effective friction angle, constrained modulus and initial shear modulus of the tested soil. DPL tests performed in the sinkhole and its surroundings allowed only the determination of the index of density of the soil. The necessity of applying different devices for soil testing in the sinkhole and its vicinity and in a distance from the sinkhole, prevented the full execution of the objectives of the research and made the comparison of the results more difficult.

Outside the sinkhole, glacial sands demonstrate relatively high values of both state and strength parameters. The average value of the index of density is 0.72, i.e. the soil is in the "dense state" and its condition varies from "medium" to "very dense". The average value of internal friction angle is 40.20.

The sinkhole development in the sands has resulted in the loosening of the soil structure. In the sinkhole, the soil is in the "loose" condition with the average value of the index of density at 0.32, and its state changes from "very loose" to "medium loose". At a depth of 4–5.5 m, there are minor voids or clusters of very loose sand of unstable structure.

The soil, both outside the sinkhole and in its interior, is characterized by changeability of state at particular depths. However, the index of density of sand in the sinkhole is significantly lower than that for the sand of undisturbed structure outside the sinkhole. This fact simplifies significantly the differentiation between the zones of undisturbed soil and zones where sinkholes formed in the past (and were then backfilled) or where the sinkhole formation process is currently in progress.

The results of soil stiffness analysis outside the sinkhole are partially ambiguous. Dilatometer tests showed the presence of high stiffness zones, in which the constrained modulus exceeded 100 MPa, as well as low stiffness zones, where the constrained modulus value fell to 8–12 MPa. The low stiffness zones coincide approximately with the occurrence of layers of sand of looser structure. The results of seismic tests disrupted the image at depths down to 2 m. At this depth, the determined values of shear modulus G_0 were considerable, i.e. of the order of 240 MPa, and at the same level the values of constrained modulus were very small, i.e. of 10 MPa order. A similar phenomenon occurred in all other SDMT tests performed in areas 3, 4 and 5, which have not been analysed in detail. The explanation of this phenomenon requires further research.

All of the CPTU and SDMT tests failed to examine the soil at depths greater than 12 m due to a high degree of compaction of glacial sands, difficulty in anchoring the rig in the slag layer that contained lumps of glass, and its insufficient power and weight. Further studies of the area should involve the determination of the values of parameters for deeper soil layers. It will require the use of more powerful devices, allowing effective anchoring of the rigs beneath the slag filling.

Finally, it should be emphasised that the presented interpretations of site investigations have been drawn with the assumption of full soil saturation. Currently, there is a lack of interpretation procedures which would consider the effect of suction in partially saturated soil. However, the results of the latest research (e.g., Pournaghiazar, et al., 2013) indicate that suction may result in significant overestimation of the values of the parameters.

The presented conclusions regarding the soil state inside the sinkhole are limited because the tests were carried out in only one sinkhole, and it would be advisable to examine other sinkholes in the study region. In the future, also non-invasive geophysical surveys over sinkholes should be performed. Such a test would enable the determination of changes of module G_0 within the sinkhole area and would allow the estimation of changes in soil bulk density caused by the sinkhole formation process.

Acknowledgements. Z. Veinović and an anonymous reviewer are thanked for their helpful remarks on the paper.

REFERENCES

Abdulla, W.A., Goodings, D.J., 1996. Modeling of sinkholes in weakly cemented sand. Journal of Geotechnical Engineering, **122**: 998–1005.

Ambrozić, T., Turk, G., 2003. Prediction of subsidence due to underground mining by artificial neural networks. Computers and Geosciences, **29**: 627–637.

Augarde, S.E., Lyamin, A.V., Sloan, S.W., 2003. Prediction of undrained sinkhole collapse. Journal of Geotechnical and Geoenvironmental Engineering, **129**: 197–205.

Betriebsbericht des Braunkohlen-Bergwerks "Cons. Grünberger Gruben" für das Jahr 1929–32 Bergrevier Görlitz, Spezial-Akten betr. Betrieb des Braunkohlenbergwerks Cons. Grünberger Gruben bei Grünberg in Schlesien, Abteilung 03, Fach B.g.3., Heft 11.

Bujkiewicz, Z., 1997. Kopalnia węgla brunatnego w Zielonej Górze (in Polish). Studia Zielonogórskie, **3**: 79-89.

Chang, K.-R., Basnett, C., 1999. Delineation of sinkhole boundary using Dutch cone soundings. Engineering Geology, **52**: 113–120.

Chudek, M., Janusz, W., Zych, J., 1988. Studium dotyczące stanu rozpoznania tworzenia się i prognozowania deformacji nieciągłych pod wpływem podziemnej eksploatacji złóż (in Polish). Zeszyty Naukowe Politechniki Śląskiej, 866, Seria Górnictwo, **141**.

Costa, Y.D., Zornberg, J.G., Bueno, B.S., Costa, C.L., 2009. Failure mechanisms in sand over a deep active trapdoor. Journal of Geotechnical and Geoenvironmental Engineering, **135**: 1741–1753.

Craig, W.H., 1990. Collapse of cohesive overburden following removal of support. Canadian Geotechnical Journal, **27**: 355–364.

Gontaszewska, A., 2011. The remains of lignite mining in Zielona Góra. In: 11 Altbergbau – Kolloquium. Wrocław, Polska, 338–348, VGE Verlag GmbH, Essen.

Gontaszewska, A., Kraiński, A., 2010. "Consolidierte Grünberger Gruben" – zarys historii (in Polish). In: Dzieje górnictwa – element europejskiego dziedzictwa kultury, 3 (eds. P.P. Zagożdżon and M. Madziarz): 111–122. Oficyna Wydawnicza Politechniki Wrocławskiej, Wrocław.

Gontaszewska, A., Kraiński, A., 2012. Deformacje powierzchni terenu na obszarze dawnego podziemnego górnictwa węgla brunatnego w okolicy Zielonej Góry (in Polish). In: Wybrane problemy badań geologicznych i hydrogeologicznych dla górnictwa i energetyki (eds. P. Bukowski): 208–219. Główny Instytut Górnictwa, Katowice.

Gutierrez, F., Guerrero, J., Lucha, P., 2008. A genetic classification of sinkholes illustrated from evaporite paleokarst exposures in Spain. Environmental Geology, **53**: 993–1006.

Iglesia, G., Einstein, H., Whitman, R., 1990. Stochastic and centrifuge modelling of jointed rock. Centrifuge modelling of jointed rock, **2**. School of Engineering. MIT, Cambridge.

ISO 14688-2:2004. Geotechnical investigation and testing. Identification and classification of soil – Part 2: Principles for a classification.

Kannan, R.C., 1999. Designing foundations around sinkholes. Engineering Geology, **52**: 75–82.

Lancellotta, R., 2009. Geotechnical engineering. 2nd ed. Taylor and Francis, London.

Lunne, T., 2001. In situ testing in offshore geotechnical investigations. Proc. Int. Conf. on In-Situ Measurements of Soil Properties and Case Histories, Bali, Indonesia: 61–78.

Lunne, T., Robertson, P.K., Powell, J.J.M., 1997. Cone penetration testing in geotechnical practice. Blackie Academic. Chapman Hall, London.

Marchetti, S., 1980. In situ tests by flat dilatometer. ASCE Journal of the Geotechnical Engineering Division, **106**: 299–321.

Marchetti, S., Monaco, P., Totani, G., Calabrese, M., 2001. The flat dilatometer test (DMT) in soil investi-gation. A Report by the ISSMGE Committee TC16. Proc. Int. Conf. on In-Situ Measurement of Soil Properties, Bali, Indonesia.

Mayne, P.W., 2007. Cone penetration testing. A synthesis of highway practice. Transportation Research Board. National Academies Press, Washington D.C.

Mayne, P.W., Coop, M.R., Springman, S., Huang, A.-B. Zornberg, J., 2009. Geomaterial behavior and testing. Proc.17th Int. Conf. SMGE. Alexandria. Millpress/IOS Press. Rotterdam, **4**: 2777–2872.

Pilecki, Z., Kotyrba, A., 2007. Problematyka rozpoznania deformacji nieciągłych dla potrzeb projektowania konstrukcji drogowych na terenach płytkiej eksploatacji rud metali (in Polish). Prace Naukowe GIG, **3**, wyd. specjalne: 379–392.

Pournaghiazar, M., Russell, A.R., Khalili, N., 2013. The cone penetration test in unsaturated sands. Geotechnique, **63**: 1209–1220.

Singh, K.B., Dhar, B.B., 1997. Sinkhole subsidence due to mining. Geotechnical and Geological Engineering, **15**: 327–341.

Stenzel, G., Melzer, K.J., 1978. Soil investigations by penetration testing according to DIN 4094.Tiefbau, **20**: 155–160.

Szafran, Z., Wróbel, I., 1975. Problemy zagospodarowania obszarów po dawnej podziemnej eksploatacji węgla brunatnego w rejonie Zielonej Góry (in Polish). Zeszyty Naukowe WSI w Zielonej Górze. Budownictwo, **29**: 149–160.

Szajna, W.St., 2013. Wykorzystanie badań nieinwazyjnych i inwazyjnych do identyfikacji lokalnych stref rozluźnienia ośrodka gruntowego (in Polish). Materiały IV Konf. Naukowej „Mechanika Ośrodków Niejednorodnych": 67–68. Oficyna Wyd. Uniwersytetu Zielonogórskiego, Zielona Góra.

Terzaghi, K., 1936. Stress distribution in dry and in saturated sand above a yielding trap-door. Proc. 1st Int. Conf. on Soil Mechanics and Foundation Engineering, Massachusetts, Cambridge: 307–311.

Tharp, T.M., 1999. Mechanics of upward propagation of cover-collapse sinkholes. Engineering Geology, **52**: 23–33.

Thomas, B., Roth, M.J.S., 1999. Evaluation of site characterization methods for sinkholes in Pennsylvania and New Jersey. Engineering Geology, **52**: 147–152.

Waltham, T., Bell, F., Culshaw, M., 2005. Sinkholes and subsidence: karst and cavernous rocks in engineering and construction. Springer, Berlin.

Whittaker, B.N., Reddish, D.J., 1989. Subsidence: Occurrence, Prediction and Control. Elsevier Science and Technology, Amsterdam.